Journal of Alzheimer's Disease 35 (2013) 179–198
DOI 10.3233/JAD-122254
IOS Press

Diabetes and Hypercholesterolemia Increase Blood-Brain Barrier Permeability and Brain Amyloid Deposition: Beneficial Effects of the LpPLA2 Inhibitor Darapladib

Nimish K. Acharya[a,e], Eli C. Levin[a,e], Peter M. Clifford[a,e], Min Han[a,e], Ryan Tourtellotte[f], Dean Chamberlain[f], Michael Pollaro[f], Nicholas J. Coretti[a,e], Mary C. Kosciuk[a], Eric P. Nagele[a], Cassandra DeMarshall[a], Theresa Freeman[b], Yi Shi[b], Chenbing Guan[c], Colin H. Macphee[d], Robert L. Wilensky[g] and Robert G. Nagele[a,*]

[a]*New Jersey Institute for Successful Aging at University of Medicine and Dentistry of New Jersey (UMDNJ) - School of Osteopathic Medicine, Stratford, NJ, USA*
[b]*Thomas Jefferson University, Philadelphia, PA, USA*
[c]*GlaxoSmithKline, Shanghai, China*
[d]*GlaxoSmithKline, King of Prussia, PA, USA*
[e]*Graduate School of Biomedical Sciences, University of Medicine and Dentistry of New Jersey, Stratford, NJ, USA*
[f]*University of Medicine and Dentistry of New Jersey - School of Osteopathic Medicine, Stratford, NJ, USA*
[g]*Hospital of the University of Pennsylvania, Philadelphia, PA, USA*

Handling Associate Editor: Thomas Shea

Accepted 13 January 2013

Abstract. Diabetes mellitus (DM) and hypercholesterolemia (HC) have emerged as major risk factors for Alzheimer's disease, highlighting the importance of vascular health to normal brain functioning. Our previous study showed that DM and HC favor the development of advanced coronary atherosclerosis in a porcine model, and that treatment with darapladib, an inhibitor of lipoprotein-associated phospholipase A_2, blocks atherosclerosis progression and improves animal alertness and activity levels. In the present study, we examined the effects of DM and HC on the permeability of the blood-brain barrier (BBB) using immunoglobulin G (IgG) as a biomarker. DMHC increased BBB permeability and the leak of microvascular IgG into the brain interstitium, which was bound preferentially to pyramidal neurons in the cerebral cortex. We also examined the effects of DMHC on the brain deposition of amyloid peptide ($A\beta_{42}$), a well-known pathological feature of Alzheimer's disease. Nearly all detectable $A\beta_{42}$ was contained within cortical pyramidal neurons and DMHC increased the density of $A\beta_{42}$-loaded neurons. Treatment of DMHC animals with darapladib reduced the amount of IgG-immunopositive material that leaked into the brain as well as the density of $A\beta_{42}$-containing neurons. Overall, these results suggest that a prolonged state of DMHC may have chronic deleterious effects on the functional integrity of the BBB and that, in this DMHC pig model, darapladib reduces BBB permeability. Also, the preferential binding of IgG and coincident accumulation of $A\beta_{42}$ in the same neurons suggests a mechanistic link between the leak of IgG through the BBB and intraneuronal deposition of $A\beta_{42}$ in the brain.

*Correspondence to: Robert G. Nagele, PhD, Professor of Medicine, New Jersey Institute for Successful Aging, University of Medicine and Dentistry of New Jersey, Stratford, NJ 08084, USA. Tel.: +1856 566 6083; Fax: +1856 566 2775; E-mail: nagelero@umdnj.edu.

ISSN 1387-2877/13/$27.50

Keywords: Alzheimer's disease, amyloid-β, autoantibodies, blood-brain barrier, cholesterol, darapladib, diabetes mellitus, immunoglobulin, lipoprotein-associated phospholipase-A_2 ($LpPLA_2$), microvasculature

INTRODUCTION

Alzheimer's disease (AD) is a progressive neurodegenerative disease that is the most common cause of dementia in the elderly [1, 2]. It is characterized pathologically by the deposition of amyloid within neurons and amyloid plaques, the appearance of neurofibrillary tangles, extensive synaptic loss, neuronal death, and reactive gliosis [3–8]. In the US, the incidence of AD is rising at an alarming rate, due in part to an increased life expectancy [1]. Despite nearly four decades of intensive research, a consensus regarding the etiology and pathogenesis of sporadic AD is still lacking, and this has greatly hampered the conception and development of effective strategies for treating and preventing this devastating disease. Recent failures of a number of drugs in clinical trials question the validity of leading models of AD pathogenesis and warrant exploration and focus on other new theories of AD pathogenesis.

A wealth of clinical and experimental evidence now suggests diabetes mellitus (DM) and hypercholesterolemia (HC) as two major risk factors for the various forms of cognitive impairment including AD [9–16]. Population-based studies have shown that DM and HC lead to increased risk of neurodegeneration, cognitive impairment, and dementia [17–23]. Although the exact nature of the mechanistic link(s) between AD, DM, and HC has not yet been elucidated, numerous studies indicate deleterious changes in the brain macro- and/or microvasculature as a key event during AD pathogenesis [24–27]. Data from brain imaging studies indicate that cerebrovascular pathology and dysfunction precede cognitive decline and the onset of neurodegenerative changes in human AD and animal models of AD [28].

DM and HC have long been known to be associated with body-wide vascular pathology and dysfunctions that include vascular inflammation, atherosclerosis, and other types of peripheral vascular disease [29–32]. In the brain, DM- and HC-associated vascular inflammation may contribute to early breakdown of the functional integrity of the blood-brain barrier (BBB) [12, 14, 33–35]. The BBB helps to maintain brain homeostasis by preventing the entry of blood components into the brain tissue that could potentially disturb the normal functioning of neurons [36, 37]. Breakdown of the BBB in AD brains is accompanied by a chronic influx of plasma components into the brain tissue, including soluble amyloid-β (Aβ) peptides, complement, serum albumin, and immunoglobulins (Igs), and this can readily be detected in postmortem brain tissue using immunohistochemistry [38–42]. In addition to disrupting brain homeostasis, the affinity of some of these plasma components (especially Igs and Aβ peptides) for neurons in AD brains may cause disturbances that favor widespread neuronal malfunction and death [40, 42]. Although a definitive role for BBB breakdown in the initiation of neurodegenerative diseases including AD has been difficult to demonstrate directly, its contribution to the progression of these diseases is more obvious and widely accepted [37, 39–43].

In a previous study, we showed that the combination of DM and HC resulted in the development of advanced atherosclerotic lesions in a porcine model, and that treatment of these diabetic-hypercholesterolemic (DMHC) animals with darapladib, an inhibitor of lipoprotein-associated phospholipase-A_2 ($LpPLA_2$), blocked the progression of atherosclerosis by inhibiting primarily the formation of necrotic cores within these lesions [44]. Interestingly, in this pig model, cursory observations of improved alertness and increased activity of darapladib-treated DMHC animals over untreated DMHC animals were also noted. Based on this, we hypothesized that chronic DMHC increases BBB permeability and that the observed behavioral differences between the two groups of animals may be due, at least in part, to beneficial effects of darapladib on the functional integrity of the BBB. To investigate this possibility, available brains from DMHC pigs with or without darapladib treatment and untreated normal controls were evaluated using quantitative immunohistochemistry in an effort to monitor the leakage of plasma components through the BBB into the brain tissue, thus reflecting BBB compromise in a diabetic and hypercholesterolemic animal model. Results showed that DMHC increased and darapladib reduced BBB permeability within the microvasculature of the cerebral cortex. We also found that IgG entering into the cortical interstitium showed preferential binding to cortical pyramidal neurons, as in AD [40, 42]. Additionally, DMHC caused increased $A\beta_{42}$ deposition in cortical pyramidal neurons throughout the brain while darapladib significantly reduced this deposition. Unexpectedly, reduction of $A\beta_{42}$ deposition was due principally to a decrease in the density of neurons

containing $A\beta_{42}$-immunopositive deposits rather than a reduction in the amount of $A\beta_{42}$ deposited in each cell. Taken together, these results suggest that a prolonged state of DM and HC may have chronic deleterious effects on the functional integrity of the BBB and that, in this DMHC pig model, darapladib reduces BBB permeability and intraneuronal amyloid deposition. In addition, the preferential binding of IgG to cortical pyramidal neurons and coincident accumulation of $A\beta_{42}$ in these same cells supports the possibility of a causal and mechanistic link between the leak of IgG through the BBB and the intraneuronal deposition of $A\beta_{42}$ in the brain as suggested previously [42]. Lastly, these results highlight the potential benefits of therapies that can block the initiation and/or progression of BBB breakdown for the treatment of neurodegenerative diseases such as AD.

MATERIALS AND METHODS

Porcine model

Full experimental details of the DMHC porcine study have been reported previously [44]. Briefly, one month after DMHC induction and animal acclimation, pigs were randomly assigned to either a control group or a treatment group receiving 10 mg/kg/d orally of the selective Lp-PLA_2 inhibitor darapladib (SB480848, GlaxoSmithKline). Three pigs did not undergo DMHC induction and acted as age-matched controls. Pigs were sacrificed 28 weeks after DMHC induction (i.e., 24 weeks after initiation of treatment). The selectivity of darapladib for human Lp-PLA_2 has been documented previously [44]. Investigators were blinded to subject group allocation. Use of these animals was approved by the IACUC of the University of Pennsylvania.

At the end of the study, pigs were euthanized and their brains were quickly removed and fixed by immersion in 10% formalin or frozen rapidly. For the neuropathological analyses, formalin fixed brains from total of 28 pigs were collected which included 13 DMHC-untreated and 12 DMHC-treated with darapladib as well as 3 untreated normal age-matched controls (control). Frozen pig brain samples were used for biochemical studies. All pigs used in this study had corresponding levels of plasma cholesterol, glucose, and Lp-PLA2 activity [44]. For the animals included in the current analysis, end of study plasma cholesterol and glucose values (average $\pm$ SD) for the DMHC control and DMHC darapladib groups were $613 \pm 331, 699 \pm 302$, and $382 \pm 110, 369 \pm 99$ mg/dl, respectively. The end of study plasma Lp-PLA2 activity (average $\pm$ SD) values for the DMHC control and DMHC darapladib groups were 88 ± 28 and 12 ± 10 nmol/min/ml, respectively.

Rodents

Normal wild-type Sprague-Dawley rats were obtained from Taconic Farms and euthanized at 7–9 weeks of age. They were maintained on *ad libitum* food and water with a 12-hour light/dark cycle in an AALAC-accredited vivarium. Animal use was reviewed and approved by the UMDNJ-SOM IACUC.

Preparation of adult rat and porcine brain proteins

Our previous studies have demonstrated that rat brain protein fractions can be used for detection of human and pig brain-reactive autoantibodies using western blots [42, 45]. In this study, rat and pig brain protein fractions were prepared. Frozen rat and pig brain samples were separately homogenized in a mixture of 1 mM phenylmethylsulfonyl fluoride, 50.0 mM Tris-HCL buffer solution, pH 7.4, at a 10.0 ml/g ratio along with protease inhibitor cocktail (Sigma-Aldrich, St. Louis, MO) at a 0.5 ml/g ratio. Using a pre-cooled Dounce homogenizer (Wheaton), brain samples were subjected to homogenization and were then centrifuged at 3,000 rpm using a Beckman CS-6R centrifuge (Beckman Coulter Inc, Brea, CA) equipped with a swing-rotor at 4°C for a period of 20 min to remove intact cells and large debris. The supernatant was retained as whole brain total protein fraction. Protein concentrations were determined using the Bradford Assay.

Detection of brain-reactive autoantibodies via western blotting

Western blot analysis was performed using rat and pig brain total protein lysates to detect the presence of brain-reactive autoantibodies in pig sera. First, 12.5% SDS-polyacrylamide separating gels were cast using the Mini PROTEAN 3 System (165-3302, BioRad, Hercules, CA) and overlain with stacking gels. 50 μg of protein sample per lane was loaded onto the gel alongside PageRuler™ Prestained Protein Ladder Plus (SM1811, Fermentas, Glen Burnie, MD). Proteins were then fractionated at 100 V for 7 min, followed by 120 V for the remainder of the resolving time. Separated proteins were then transferred to Hybond-ECL Nitrocellulose Membrane (RPN3032D, Amersham, Piscataway, NJ) for 40 min at a constant voltage of 100 V.

Blots were blocked in 5.0% non-fat dried milk dissolved in PBS-Tween (PBS-T) buffer and then transferred to pig serum samples (primary antibody), diluted 1 : 500 in blocking solution, for overnight incubation at 4°C. Blots were then thoroughly rinsed in PBS-T buffer and placed in peroxidase-conjugated secondary antibody (Anti-pig IgG, AbD Serotec, AAI41P, dilution 1 : 50,000) and incubated for 1 h at 4°C. They were then thoroughly rinsed in PBS-T and quickly rinsed in dH_2O to remove phosphate buffer. Blots were then developed using SuperSignal West Femto Maximum Sensitivity Substrate (Thermo Scientific/Pierce, IL, USA) and autoradiographed. Each western blot for a given serum sample was performed in triplicate.

Preparation of pig brain tissue for morphological analyses

Each pig brain was subdivided anteroposteriorly into anterior, middle, and posterior regions, and the cerebral cortex from each region was prepared for routine paraffin embedding, histological sectioning, and immunohistochemistry. Each brain specimen was oriented and sectioned so as to maximize the amount of tissue available for quantification. During this study, we focused on the cerebral cortex because this is one of the brain regions that undergoes AD-related neurodegenerative changes. Total areas of the cerebral cortex were measured in hematoxylin- and eosin-stained sections using Image Pro Plus (Phase 3 Imaging, Glenn Mills, PA).

Immunohistochemistry

Immunohistochemical analysis of brain tissue was carried out as previously described [42, 46, 47]. Tissues were deparaffinized using xylene and rehydrated through a graded series of decreasing concentrations of ethanol. Antigenicity was enhanced by microwaving sections in citrate buffer. Endogenous peroxidase was quenched by treating sections with 3% H_2O_2 for 10 min. Sections were incubated in appropriate blocking serum and then treated with primary antibodies [biotinylated anti-swine IgG (Vector Laboratories, Inc., Burlingame, CA; Catalogue BA-9020, dilution 1 : 100) or anti-$A\beta_{42}$ (Millipore Corporation, Billerica, MA; Catalogue # AB5078P; dilution 1 : 50)] for 1 h at room temperature. The specificity of the antibodies used has already been verified [48–50]. After a thorough rinse in PBS, sections probed with anti-$A\beta_{42}$ were then probed with biotin-labeled secondary antibody (anti-rabbit IgG, Vector Laboratories, Inc.; Catalogue PK-6101, dilution 1 : 100) for 30 min. After thorough rinse in PBS, sections were treated with the avidin-peroxidase complex (Vectastain ABC Elite kit, Vector Laboratories, Inc.; Catalogue PK-6100) and visualized with 3-3-diaminobenzidine-4-HCL (DAB)/H_2O_2 (Imm-PACT-DAB) (Dako, Carpinteria, CA, DAB chromogen system, Code K3468). Sections were then lightly counterstained with hematoxylin, dehydrated through increasing concentrations of ethanol, cleared in xylene, and mounted in Permount (Fisher Scientific). Immunoreactions and antigenicity were tested using controls that included brain sections treated with non-immune serum or omission of the primary antibody. Specimens were examined and photographed with a Nikon FXA microscope, and digital images were recorded using a Nikon DXM1200F digital camera and analyzed using Image Pro Plus (Phase 3 Imaging) and Cell Profiler (BROAD Institute).

Detection and quantification of the leak of IgG from brain blood vessels as an indicator of BBB permeability

Sections containing the cerebral cortex were immunostained with antibodies specific for pig IgG to detect and localize nonvascular IgG both free in the brain interstitial space and associated with neurons and astrocytes. Since, in normal healthy animals, IgG tends to be excluded from the brain parenchyma by virtue of the integrity of the BBB, we therefore interpreted the presence of free interstitial IgG, IgG-immunopositive perivascular leak clouds, and IgG associated with neurons and astrocytes as evidence of local plasma leaks and increased BBB permeability [40, 42, 51]. We calculated the density of vascular leaks in the cerebral cortex as the number of detectable leaks per unit area. To accomplish this, we first measured the total area (in mm^2) of cerebral cortex represented in each hematoxylin- and eosin-stained section using Image Pro Plus. Consecutive sections were then immunostained as described above with anti-swine IgG antibodies to detect the presence of IgG. Blood vessels containing IgG-positive plasma served as positive internal controls. Each immunostained section was evaluated by counting the total number of profiles of blood vessels appearing in the cortex that also displayed perivascular leak clouds. Only leak clouds containing blood vessel profiles were included in the count so that the source vessel could be classified as an arteriole, capillary, or venule. The density of leaks was calculated as the number of leaks per unit area (mm^2) of cortex or non-cortex appearing in the sections.

Quantitative analysis of the extent of vascular (BBB) leaks

A relative scale was developed to quantify the extent of each leak (Fig. 3c–h). Based on the relative size of each leak cloud, a score was given that correlated with the extent of vascular leakage and BBB breakdown. Individual leak clouds appearing in brain histological sections were scored for the extent of the leak in specific regions of the brain. It should be noted here that, although perivascular leak clouds generally appear as circular with the source blood vessel at or near the center, these clouds are actually cylindrical in three-dimensions. Thus, a doubling of the diameter of the leak cloud as seen in sections translates into a roughly four-fold increase in the volume of the leak cloud.

Quantitative analysis of the amount and distribution of $A\beta_{42}$ peptide throughout the cerebral cortex of the pig brain

Sections were immunostained with antibodies specific for $A\beta_{42}$ and examined and photographed with a Nikon FXA microscope. Images were recorded using a Nikon DXM1200F digital camera and analyzed using Image Pro Plus (Phase 3 Imaging) and Cell Profiler. At each of five randomly selected locations within the cerebral cortex, four 20× images were taken; two from the superficial cerebral cortex layers 2–3 (upper cortex) and two from the corresponding deeper cortical layers 4–6 (deeper cortex). In this way, a total of twenty 20× images were obtained from each slide. For image analysis, an automated subprogram operating within the Image Pro Plus image analysis program was used. Control images showing little or no $A\beta_{42}$ immunoreactivity were used to set the baseline threshold under conditions of identical light intensity, light filters, condenser and aperture settings, and photoamplification by the digital camera. Total $A\beta_{42}$ present in each 20× histological section was measured automatically and the data was downloaded into an excel spreadsheet and analyzed.

Statistics

Statistical significance was determined by the Student's t test, and $p < 0.05$ (*) was considered statistically significant. Standard error was used to represent the variations within each treatment group.

RESULTS

The effects of prolonged (6 months) DMHC on BBB permeability to IgG and $A\beta_{42}$ deposition in the cerebral cortex of pig brains were studied using immunohistochemistry carried out on histological sections from the following subject groups: DMHC controls, darapladib-treated DMHC, and normal, non-DMHC controls (Control). Anti-pig IgG and anti-$A\beta_{42}$ antibodies were used to detect the following AD-relevant features and parameters among these subject groups: the location, frequency, and extent of BBB breach and permeability; the binding of extravascular IgG to cells and other elements within the brain parenchyma and $A\beta_{42}$ localization and deposition in the brain.

The presence of substantial IgG in the parenchyma of the cerebral cortex is a sensitive and reliable indicator of local BBB breakdown

An intact BBB restricts what enters into the brain interstitial space from local blood vessels. The stringency of this restriction varies considerably in different brain regions, with the cerebral cortex showing relatively high stringency. One class of molecules that is effectively excluded from the cerebral cortex is immunoglobulin (Ig). Under conditions of BBB breakdown, IgG, along with most other plasma components, can escape from blood vessels and enter into the brain interstitial space [38–42]. In the present study, we used immunohistochemistry and anti-pig IgG antibodies to probe for the presence of interstitial IgG as a visual indicator of local BBB breakdown and vascular leak. Fig. 1a and b show typical regions of the cerebral cortex of normal, non-DMHC control pig brains where IgG is largely confined to the microvasculature (arterioles, venules, and capillaries). Neurons and non-neuronal (glial) cells are mostly IgG-negative. By contrast, IgG-positive microvascular leaks are more commonly observed in the cerebral cortex and hippocampus of DMHC pigs (Fig. 1c–g). Variations observed in the number and extent of blood vessel leaks support the stochastic nature of these leaks. The size and shape of perivascular leak clouds observed in histological sections closely reflected the size and orientation of the source blood vessels with respect to the section plane. Among the smallest arterioles and capillaries, the coincident spatial association of smaller, IgG-positive leak clouds with blood vessels confirms these vessels as the source of the IgG within the leak cloud (Fig. 1c–f). Interestingly, a rather sharp interface between IgG-positive and negative zones of the cerebral cortex was frequently observed (Fig. 1d–e). In addition, when the source vessels were not contained within the section

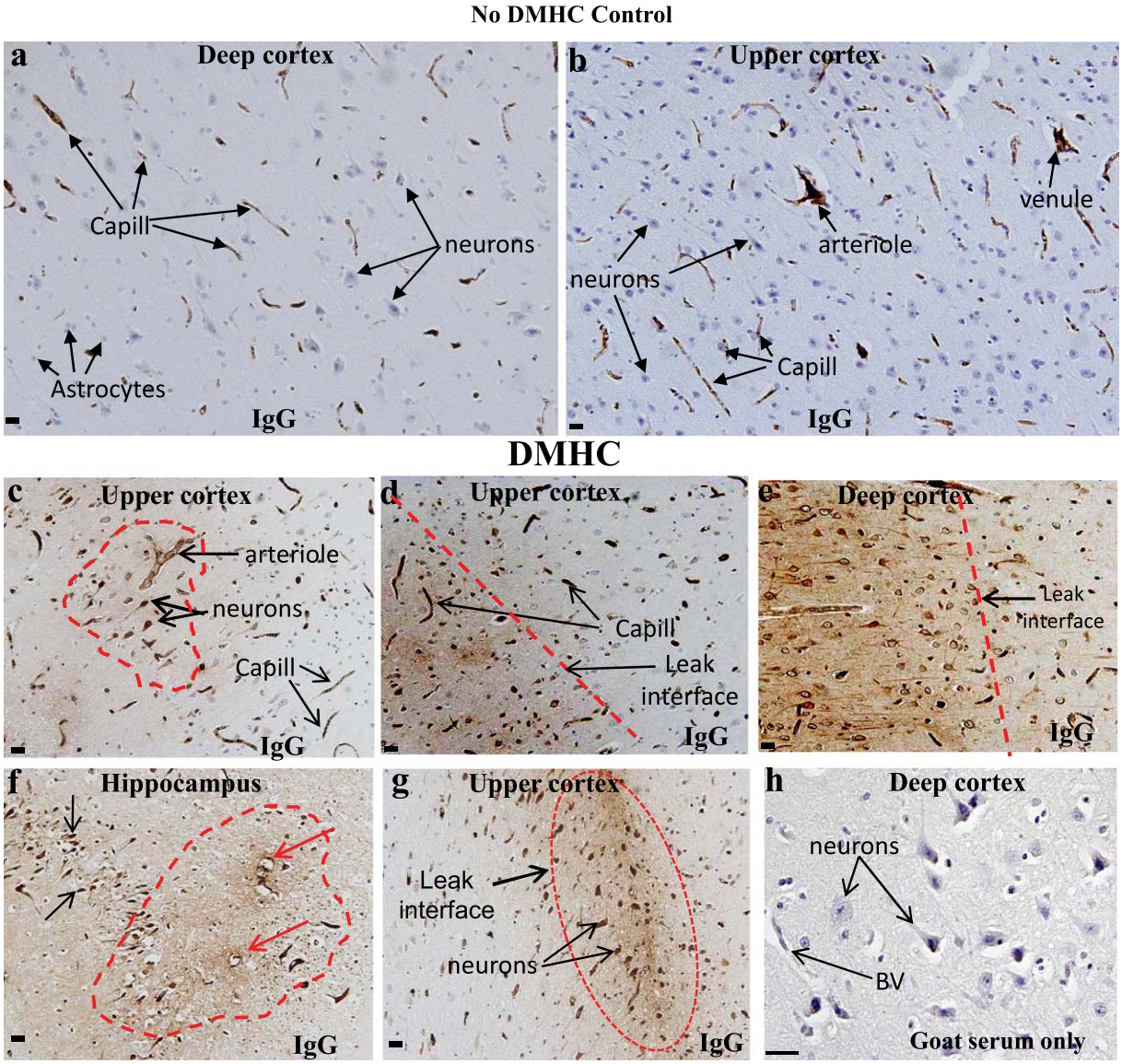

Fig. 1. IgG-positive microvascular leaks are commonly observed throughout the cerebral cortex of DMHC pigs. a, b) Regions of the cerebral cortex of non-DMHC control pig brains where IgG staining (brown color) is confined to the microvasculature (arterioles, venules, and capillaries). c–h) Regions of cerebral cortex of DMHC control pig brains showing several examples of IgG-positive microvascular leaks. Some leaks are more focal with an obvious source vessel (c and f). In others, leak clouds form rather sharp borders or interfaces where IgG-positive immunostaining abruptly stops (d, e, and g). Neurons (dark brown spots) are intensely IgG-positive in regions of leakage (c, e, and g). Capill, capillary; BV, blood vessel. Scale bar = 50 μm.

plane, small isolated leak clouds or linear tracts of IgG-positive material were often seen without apparent source vessels (Fig. 1g). Sections probed with the blocking sera, goat IgG (Fig. 1h) lacked detectable immunostaining. Together, these observations suggest that the presence of IgG in the brain interstitium provides an effective and reliable biomarker for local BBB dysfunction as has been suggested previously [38–41].

Within the microvasculature, arterioles are the main source of plasma components that leak into the brain

BBB breakdown was observed in all major categories of blood vessels that comprise the microvasculature (i.e., arterioles, venules, and capillaries; Fig. 2). However, using IgG as an indicator of BBB breach, arterioles were clearly the predominant

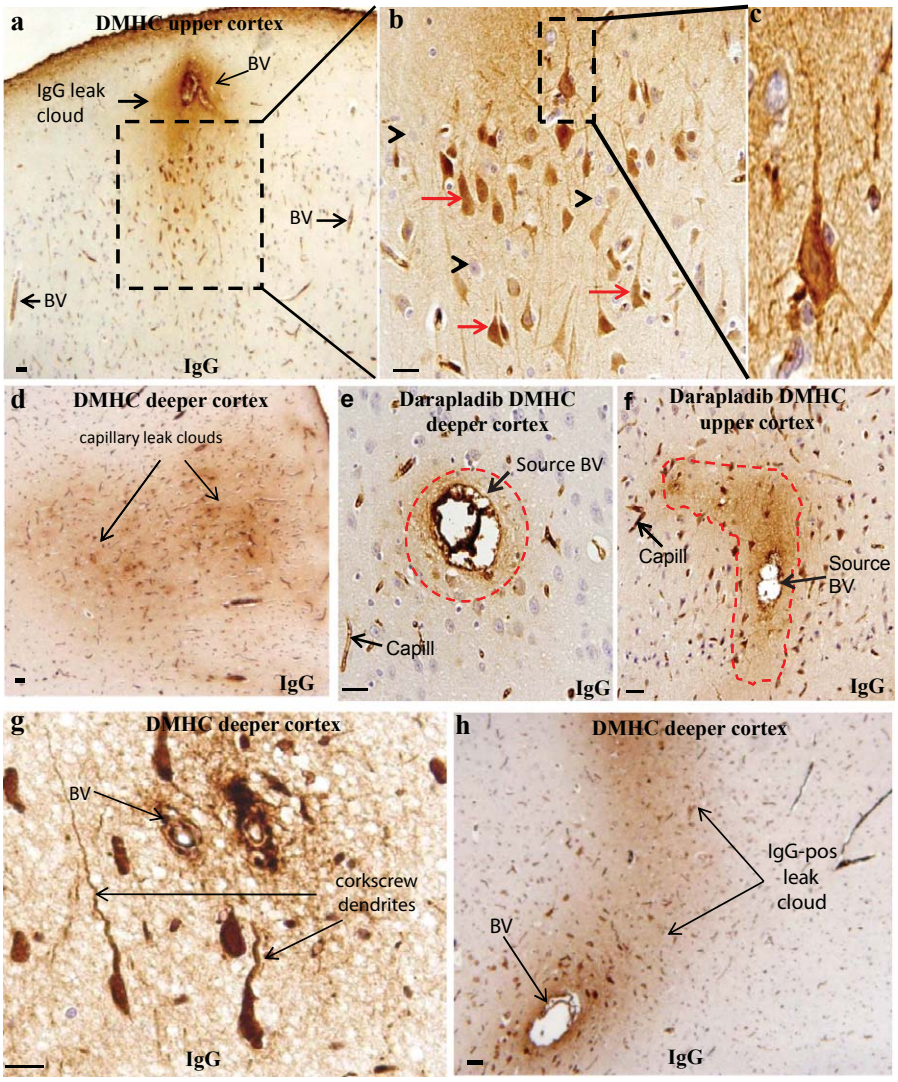

Fig. 2. Histological sections of the cerebral cortex of DMHC control and darapladib-treated DMHC pigs showing several examples of leaks associated with arterioles and capillaries with surrounding IgG-positive neurons. Arterioles form prominent perivascular leak clouds and are primary contributors to the total amount of leaked components that enter into the brain (a–c, e, f, and h). Capillaries can also form small leak clouds that contribute to a region of diffuse IgG-positive staining (d). Neurons (red arrows) within perivascular leak clouds are strongly and selectively IgG-positive (b), and those that are the most intensely IgG-positive frequently exhibit "corkscrew dendrites" indicative of dendrite instability and collapse (b and g). Capill, capillary; BV, blood vessel. Scale bar = 50 μm.

contributors of plasma components that leaked from blood vessels into the brain interstitium (Fig. 2a, e–f, h). This most often appeared as perivascular IgG leak-clouds (Fig. 2a, e–f, h). The apparent predominance of arterioles is most likely due to the fact that, among the different types of blood vessels that comprise the brain microvasculature, only arterioles are under a constant positive pressure. For this reason, even if the BBB is equally permeable in arterioles, venules, and capillaries throughout the cortical microvasculature, it is likely that arterioles would still appear to be the most permeable type of blood vessel because of their increased positive pressure compared to capillaries and venules. Figure 2d shows a portion of a small capillary bed in which IgG-positive material appears to be leaking from several adjacent capillaries, collectively contributing to a more diffuse distribution of plasma components (including IgG) in the surrounding brain tissue.

Neurons in the vicinity of perivascular leak clouds are selectively IgG-immunopositive and IgG binding may be associated with local dendrite collapse and loss of synapses

The cell body and dendrite branches of neurons located within the borders of perivascular leaks cloud were often strongly and selectively IgG-positive, whereas those well outside of leak clouds were mostly IgG negative, with the intensity of IgG-positive immunostaining gradually decreasing with increasing distance from the leak cloud and its source vessel (Fig. 2a–f, h). In addition, the relative intensity of neuronal IgG immunostaining often greatly exceeded that of the "free" IgG in the surrounding extracellular space, suggesting that IgG has a greater affinity for neurons than for other nearby brain elements (Fig. 2b, c). Interestingly, cortical pyramidal neurons throughout the cerebral cortex clearly showed the greatest propensity for binding of IgG (Fig. 2b, c, e–g). However, the number of IgG-positive neurons within perivascular plasma leak clouds was highly variable even within the same treatment groups. Many of the most intensely IgG-positive neurons exhibited conspicuous morphological alterations in their main dendrites, taking on a "corkscrew" appearance consistent with dendrite collapse and retraction (Fig. 2b, c, g). When IgG-positive and IgG-negative neurons were found to coexist within a single perivascular leak cloud, these neurons only rarely exhibited corkscrew dendrites (Fig. 2e). By contrast, when all neurons in the vicinity of a vascular leak were intensely IgG-positive, many IgG-positive neurons exhibited corkscrew dendrites indicating dendrite degeneration and retraction (Fig. 2b, c, g). The corkscrew dendrites are probably due to the helical arrangement of neurofilaments contained within them. This further suggests that the amount of local neuronal pathology (i.e., dendrite collapse and synaptic loss) may be directly proportional to the intensity of local neuronal IgG immunolabeling. Unexpectedly, despite neurons in DMHC pig brains frequently exhibiting evidence of dendrite trunk retraction, other typical features associated with local neuronal cell death were not observed, and this was consistent with the lack of microglial activation in DMHC pig brain tissue (data not shown).

DMHC increases and darapladib reduces the leak of IgG through the BBB

To determine the effects of DMHC and darapladib on the number of vessels involved in BBB breakdown and plasma leak, we counted the total number of blood vessels exhibiting detectable leaks per unit area of cerebral cortex in each of the three subject groups and also measured the relative extent of the leak (Fig. 3a, b). As mentioned above, perivascular leak clouds were observed in all three types of vessels that make up the cerebral microvasculature (arterioles, venules, and capillaries). As represented in Fig. 2a–f, the total density of microvascular leaks (number per unit area of cerebral cortex) was found to be numerically higher in the DMHC pig (DMHC Control) cortex than in darapladib-treated DMHC (DMHC Darapladib) and normal controls (Fig. 3a). Although darapladib reduced the number of leaking vessels, this reduction did not reach statistical significance (Fig. 3a). We also determined the effects of DMHC and darapladib on the extent of each leak (i.e., the amount of leaked IgG-positive material per unit area of cortex) using a scoring system that we devised to represent the extent of leak occurring at each site (Fig. 3c–h). For each section of brain tissue evaluated, the individual "leak extent" values for each cortical blood vessel leak were added to generate a "total leak" value for the cortex in each specimen. This total leak value was divided by the area of the cortex in mm^2, thus allowing expression of the extent of cortical leak as "extent of leak per mm^2 of cortex". Using this approach, untreated DMHC (DMHC Control) pig brains showed a greater extent of BBB permeability and vascular leak than either the darapladib-treated DMHC (DMHC Darapladib) or non-DMHC control pig brains (Controls), with darapladib having the effect of reducing the extent of the vascular leak to a level approaching that of non-DMHC controls (Fig. 3b). This enhanced arteriolar permeability in brains of DMHC pigs observed here is similar to that seen in the arterioles of AD brains [40, 42, 45].

Brain-reactive autoantibodies are abundant in pig sera

As described above, extravasation of IgG was directly observed in histological sections of the cerebral cortex as focal perivascular leak clouds or as areas of more diffuse IgG-positive immunostaining presumably emanating from blood vessel sources located above or below the histological section plane. We have also demonstrated that IgG binds selectively to brain neurons, especially pyramidal neurons. These findings imply that brain-reactive (including neuron-binding) autoantibodies are abundant in the blood of pig. To further examine this possibility, we carried out

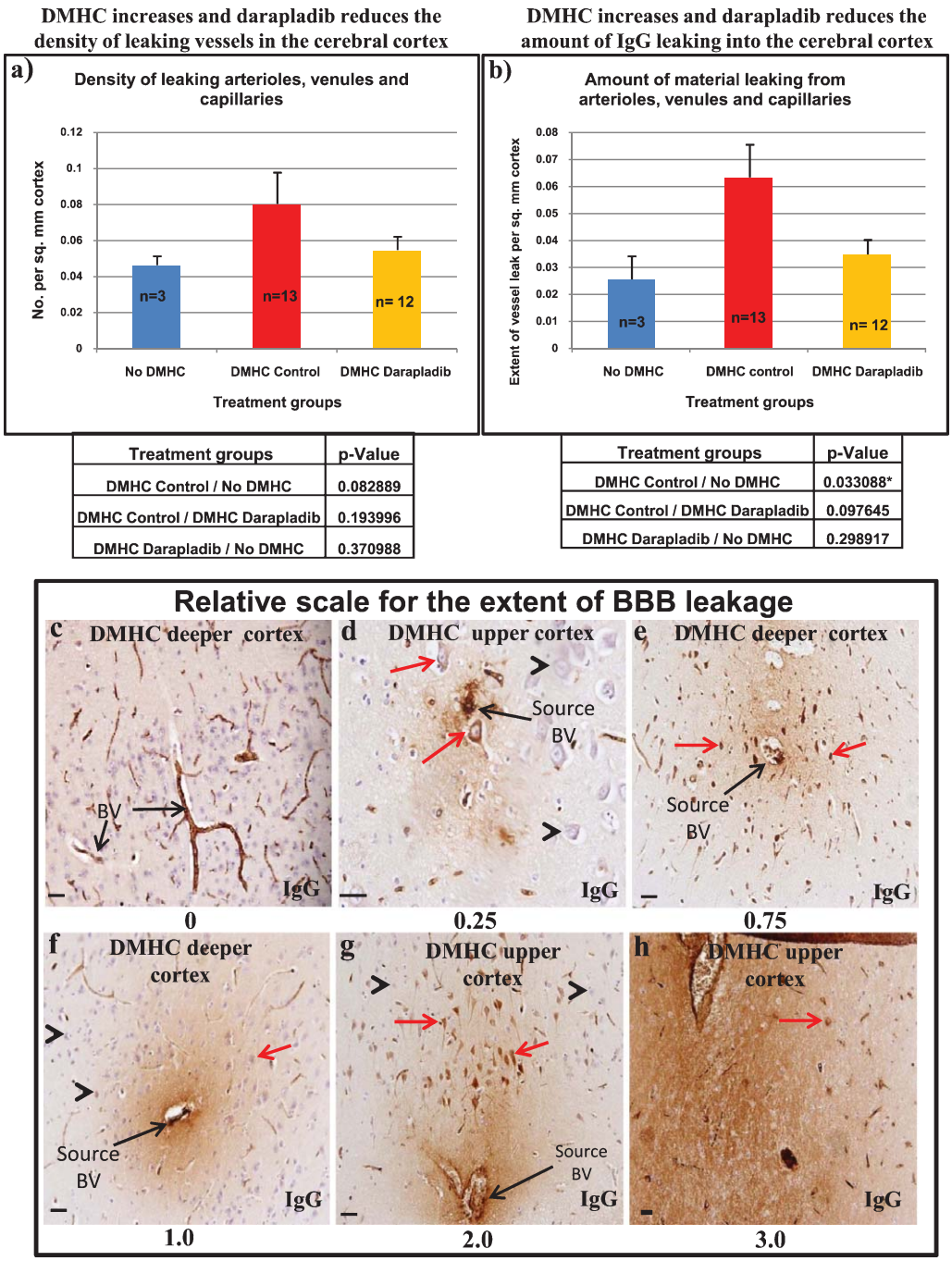

Treatment groups	p-Value
DMHC Control / No DMHC	0.082889
DMHC Control / DMHC Darapladib	0.193996
DMHC Darapladib / No DMHC	0.370988

Treatment groups	p-Value
DMHC Control / No DMHC	0.033088*
DMHC Control / DMHC Darapladib	0.097645
DMHC Darapladib / No DMHC	0.298917

Fig. 3. Darapladib reduces the leakage of IgG through the BBB. a) Graph showing that the total density (number per unit area of cerebral cortex) of microvascular leaks from brain blood vessels was numerically higher in the DMHC pig brain cerebral cortex (DMHC Control) than in darapladib-treated DMHC (DMHC Darapladib) animals and untreated controls (No DMHC). b) Graph showing the effects of DMHC and darapladib on the amount of leaked IgG-positive material per unit area of cortex using a scoring system (c–h) developed to reflect the extent of each detected leak. Individual "extent values" for each cortical leak were added together to generate a "total leak extent value" for the cortex in each specimen. This total leak extent value was divided by the area of the cortex in millimeters to express the extent of cortical leak as "extent of leak per sq. mm of cortex". DMHC pig brains showed a greater extent of vascular leak than either the darapladib-treated DMHC or untreated control pig brains, with darapladib reducing the extent of the leak to a level approaching that of No DMHC controls. Red arrows, IgG positive neurons; Black arrow head, pyramidal neuron devoid of IgG immunolabeling; BV, blood vessel. Scale bar = 50 μm.

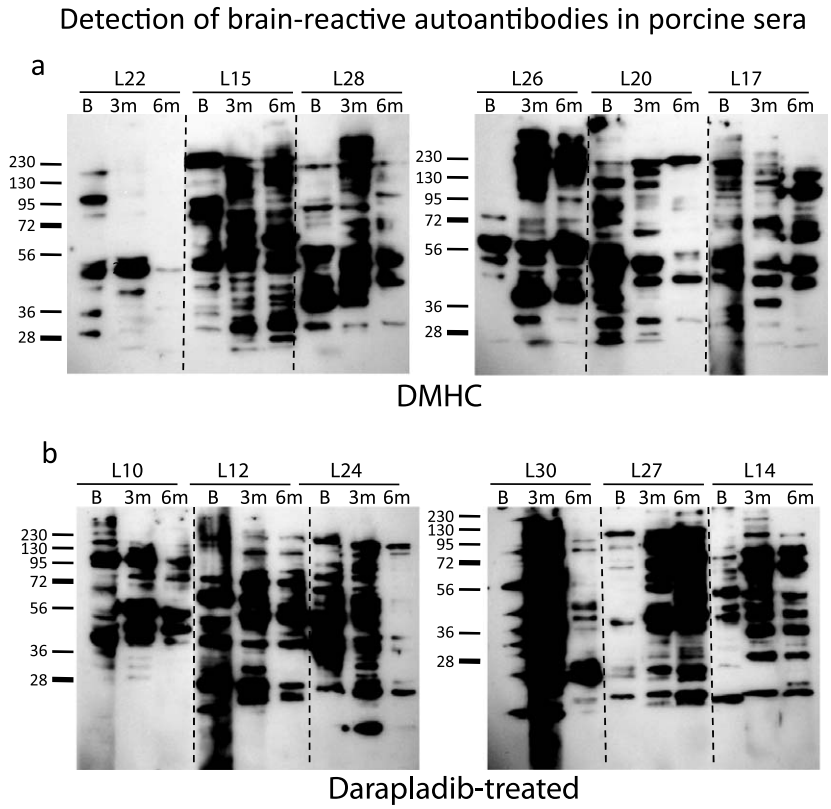

Fig. 4. Western analysis showing that brain-reactive autoantibodies are abundant in porcine sera. Rat brain proteins obtained from total brain homogenate were probed with individual pig sera from the two treatment groups (DMHC and DMHC-treated with darapladib) and at three different timepoints (baseline, 3 months, and 6 months). a, b) Western blots that demonstrate the abundance of brain-reactive autoantibodies in pig sera. Most sera had comparable levels of brain-reactive autoantibodies at baseline. The majority of pig sera showed an increase in the number and titer of brain-reactive autoantibodies at the 3 month time point. Pig sera differed in the amount of brain-reactive autoantibodies at the 6 month time point compared with the 3 month time point: 3 of 8 DMHC-only sera (L22, L28, L20) showed a decreased overall number and amount of brain-reactive autoantibodies at the 6 month time point; whereas 6 of 8 sera from darapladib-treated DMHC pigs (L10, L12, L24, L30, L14, L9) showed decreases. Results suggest that darapladib reduces somewhat the number and amount of brain-reactive autoantibodies in the DMHC model over a treatment period of six months. The number above each lane is the individual pig identity number and, just under this number, is the time point in months at which the blood sample was taken (B, baseline; 3 m, 3 months; 6 m, 6 months). Baseline refers to the time point where treatment of streptozotocin-induced diabetic pigs with darapladib was initiated.

western analyses of sera obtained from the animals used in this study using methods described previously for human sera [42, 45]. Rat brain proteins obtained from brain homogenate were probed with identical dilutions (1 : 500) of individual pig sera from DMHC and darapladib-treated DMHC groups and at three timepoints (baseline, 3 months, and 6 months). Figure 4 shows representative examples of the resulting western blots and confirms the abundant presence of brain-reactive autoantibodies in all pig sera, with each immunopositive band presumably representing at least one brain-reactive autoantibody. Most autoantibodies persisted in sera throughout the treatment period, although the titers of individual autoantibodies varied somewhat and some new autoantibodies appeared during the treatment period. Interestingly, the majority of sera showed an increase in the number and titer of brain-reactive autoantibodies over baseline at the 3 month time point. Also, individual sera were found to differ in the relative amount of brain-reactive autoantibodies at the 6 month timepoint compared with the 3 month timepoint: with 3 of 8 sera tested from the DMHC group showing a decreased overall number and amount of brain-reactive autoantibodies, whereas 6 of 8 sera from darapladib-treated DMHC pigs showed decreases (Fig. 4a, b). These qualitative results suggest that darapladib reduces somewhat the number and amount of brain-reactive autoantibodies in the DMHC model over the treatment period of six months.

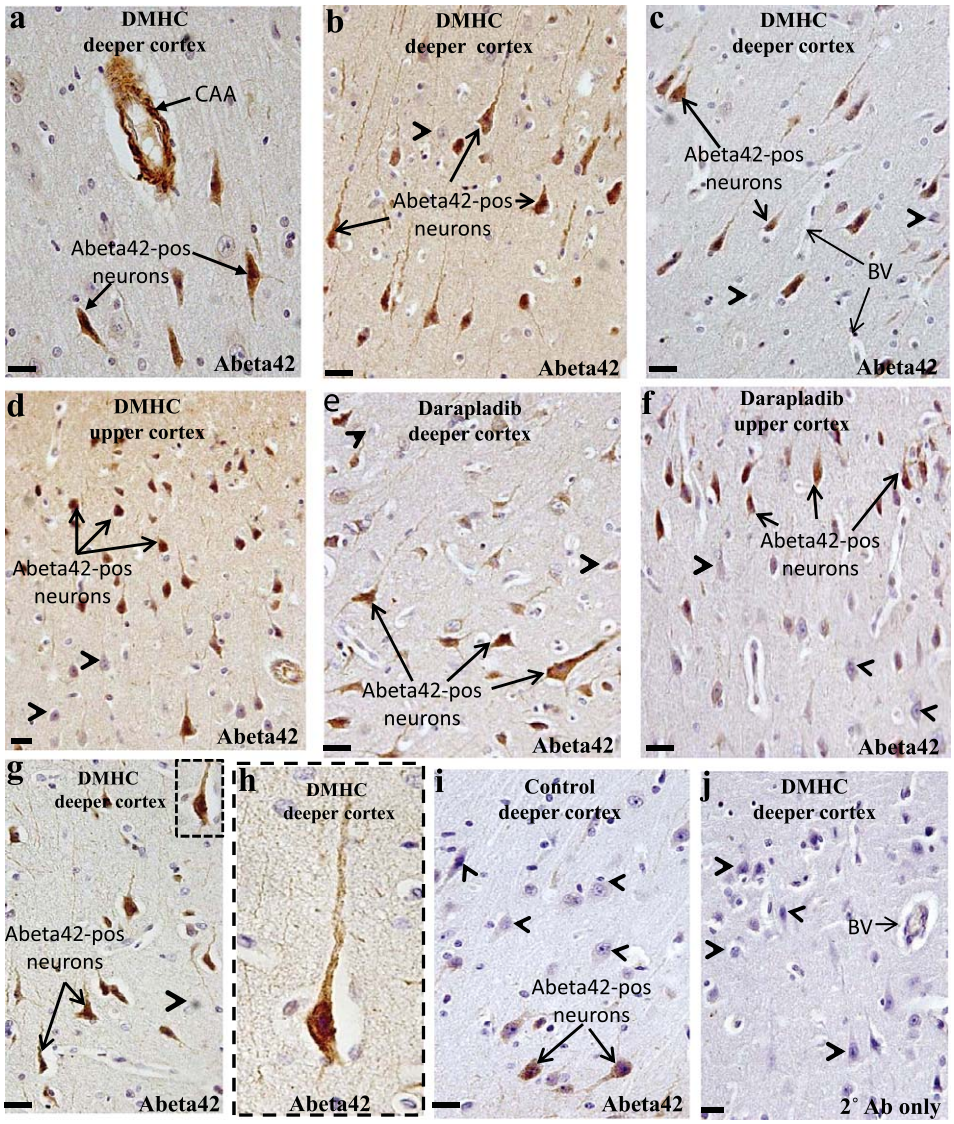

Fig. 5. $A\beta_{42}$ accumulates selectively in pyramidal neurons and occasionally in arterioles in the cerebral cortex. a) Section showing several pyramidal neurons in the vicinity of an arteriole with $A\beta_{42}$-immunopositive vascular smooth muscle cells. b–h) Sections showing the selective localization of $A\beta_{42}$-immunopositive material within pyramidal neurons. h) $A\beta_{42}$-positive immunoreactivity was largely restricted to the neuronal perikaryon or cell body and main dendrite trunk of these neurons. i) Section of No DMHC control cerebral cortex showing minimal IgG-positive material in the neurons. j) Section of cerebral cortex from DMHC control treated with secondary antibody only, an example of a negative immunohistochemical control. Black arrow head, pyramidal neuron devoid of IgG immuno-labeling; CAA, cerebral amyloid angiopathy; BV, blood vessel. Scale bar = 50 μm.

$A\beta_{42}$ accumulates selectively in pyramidal neurons

In the cerebral cortex, large and small pyramidal neurons dominate and tend to be distributed into several loosely demarcated layers. In histological sections immunostained to reveal the localization and distribution of $A\beta_{42}$ peptide, occasional $A\beta_{42}$-immunopositive blood vessels were observed, suggesting some cerebrovascular amyloidosis (Fig. 5a). However, outside of these vessels, essentially all detectable $A\beta_{42}$ within the brain parenchyma was confined to neurons, and the dominant $A\beta_{42}$-positive neuronal cell type was the pyramidal neuron (Fig. 5b–f). The reason for this remarkable selectivity of $A\beta_{42}$ for pyramidal neurons is unknown, but it is interesting that this is the same type of neuron that is well-known to accumulate excessive $A\beta_{42}$ and is also

IgG-immunopositive in human AD brains [42, 47]. Pyramidal neurons in both upper and deeper regions of the cerebral cortex were commonly $A\beta_{42}$-positive in both the cell body and along substantial lengths of the main dendrite trunk (Fig. 5a–h). Though most pyramidal neurons were immunoreactive for $A\beta_{42}$, some pyramidal neurons devoid of $A\beta_{42}$ labeling were also present (black arrowheads). The number of $A\beta_{42}$ positive neurons declined from DMHC to Darapladib-treated DMHC to controls (Fig. 5b–i). In the cortex of all treatment groups, glial cell-associated $A\beta_{42}$ was not detected. Immunohistochemical control sections probed with blocking sera, goat sera (data not shown), or with secondary antibody (anti-rabbit IgG) only were negative, thus confirming the specificity of the staining reaction (Fig. 5j).

DMHC increases and darapladib reduces the density of $A\beta_{42}$-positive neurons and the total brain $A\beta_{42}$ load in the DMHC pig cerebral cortex

We next determined the effects of DMHC with or without darapladib treatment on the deposition of $A\beta_{42}$ in the pig brain. To accomplish this, brain sections were immunostained using anti-$A\beta_{42}$ antibody, imaged, and subjected to image analysis. Measured parameters included the number of $A\beta_{42}$-positive neurons per unit area (density) and the total amount of $A\beta_{42}$ load per unit area of brain tissue by counting pixels attributable to $A\beta_{42}$. It should be noted here that, as shown above via immunohistochemistry, essentially all $A\beta_{42}$-postive material was contained within neurons, particularly pyramidal neurons, similar to what is seen in AD brains at earlier stages of the disease. DMHC was found to increase the density of $A\beta_{42}$-positive neurons in the cerebral cortex compared to untreated normal controls, and treatment of DMHC animals with darapladib significantly lowered the density of $A\beta_{42}$-positive neurons in the cerebral cortex to levels comparable to untreated non-DMHC controls (Fig. 6a). We next asked if the effects of DMHC on intraneuronal $A\beta_{42}$ were uniform among all pigs in the DMHC subject group. Figure 6b presents the data for individual pigs as a histogram and shows that the DMHC condition increased the density of $A\beta_{42}$-positive neurons in most of the pigs belonging to this group while the density of $A\beta_{42}$ positive neurons in a majority of DMHC pigs treated with Darapladib was comparable to that of normal controls. Interestingly, the individual animal data is particularly informative because it suggests that the condition of DMHC does not affect all animals equally, and that there may be an "all or none" response to the DMHC condition in terms of neuronal $A\beta_{42}$ deposition within the brains. In this case, half of the animals are apparently affected and show increased intraneuronal $A\beta_{42}$ deposition and the other half of the animals show resistance to this effect of DMHC. Treatment with darapladib resulted in an overall reduction in the density of $A\beta_{42}$-positive neurons in the cerebral cortex of DMHC pigs (Fig. 6a, b). The individual pig data suggests that darapladib may somehow block conditions that trigger increased $A\beta_{42}$ deposition within neurons in the cerebral cortex (Fig. 6b). To determine if the effects of DMHC and darapladib extend to different layers of the cerebral cortex, we compared the densities of $A\beta_{42}$-positive neurons in the smaller pyramidal neuron layers of the upper or more superficial layers of the cerebral cortex with the larger pyramidal neurons occupying deeper layers. In both neuronal populations, DMHC was found to similarly increase and darapladib to reduce the number of pyramidal neurons that were $A\beta_{42}$-positive (Fig. 6c). Lastly, we compared the total brain load of $A\beta_{42}$ among the different treatment groups. Although, unfortunately, the normal controls showed widely divergent levels of $A\beta_{42}$ in the brain for unknown reasons that becomes particularly problematic with a small subject "*n*", comparison of the two other subject groups revealed that darapladib caused a significant reduction in total $A\beta_{42}$ load in the cerebral cortex of DMHC pigs (Fig. 6d).

Most of the IgG labeled pyramidal neurons also accumulate $A\beta_{42}$

As demonstrated above, extravasated IgG binds selectively to pyramidal neurons populating the cerebral cortex, and these are the same neuronal subtype that also shows intracellular $A\beta_{42}$ deposition. This coincidence raises the possibility that there might be a mechanistic link between the binding of IgG to the surfaces of neurons and $A\beta_{42}$ deposition. To examine this possibility, we carried out immunohistochemistry on consecutive sections of cerebral cortex from DMHC and DMHC darapladib animals (Fig. 7). Results showed co-localization of IgG and $A\beta_{42}$ in the majority of pyramidal neurons in both subject groups (thick black arrows and encircled). Glial cells lacked immunoreactivity to IgG and $A\beta_{42}$ (Fig. 7a–d).

DISCUSSION

DM and HC are now considered to be major risk factors for AD [9–12, 20, 23, 35, 52]. Since most of the patients diagnosed with DM also have HC, a close

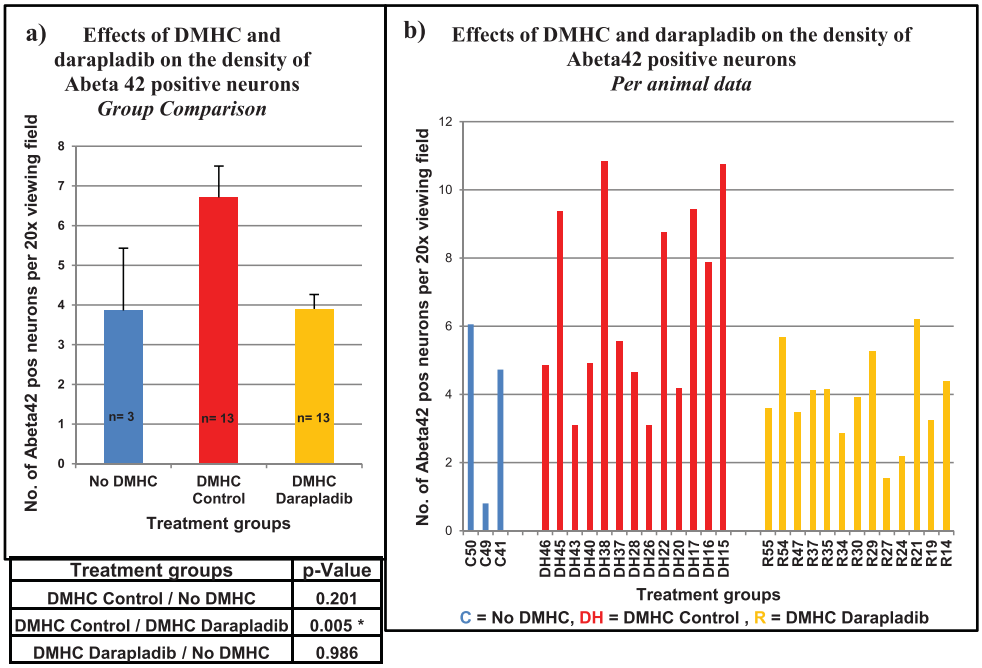

Treatment groups	p-Value
DMHC Control / No DMHC	0.201
DMHC Control / DMHC Darapladib	0.005 *
DMHC Darapladib / No DMHC	0.986

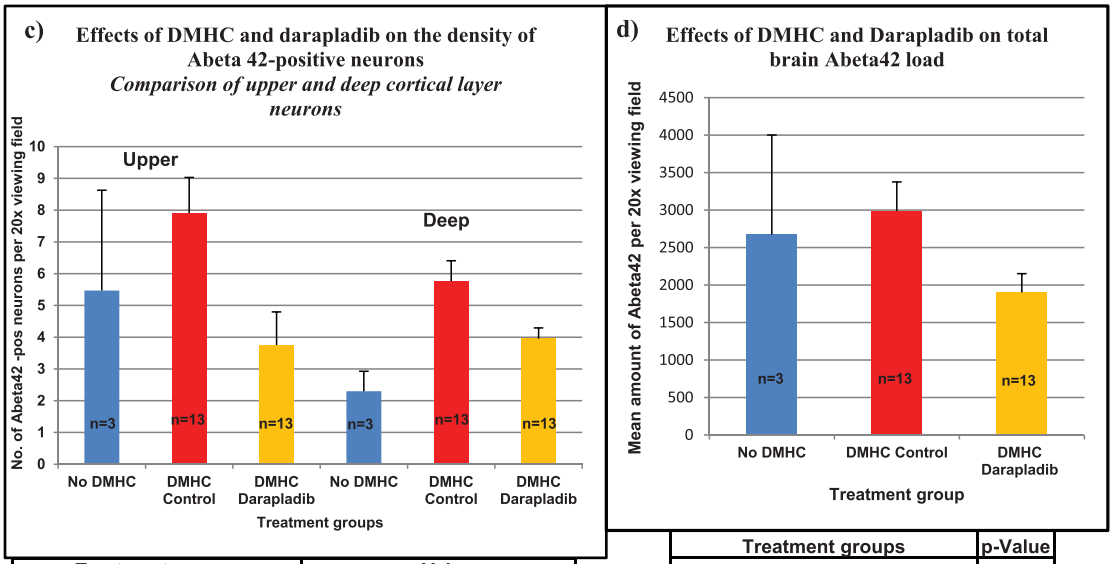

Treatment groups	p-Value	
	Superficial layer	Deep layer
DMHC Control / No DMHC	0.503062483	0.006205543 *
DMHC Control / DMHC Darapladib	0.006508613 *	0.023602109 *
DMHC Darapladib / no DMHC	0.576638997	0.095876926

Treatment groups	p-Value
DMHC Control / No DMHC	0.839
DMHC Control / DMHC Darapladib	0.029 *
DMHC Darapladib / No DMHC	0.622

Fig. 6. Quantitative analysis revealing the effect of DMHC and darapladib on the density of $A\beta_{42}$-positive neurons and $A\beta_{42}$ accumulation in pig cerebral cortex. a) Pooling of data from individual animals into the three subject groups revealed that darapladib causes a significant reduction in the density of $A\beta_{42}$-positive neurons in the cerebral cortex of DMHC pigs. b) A histogram with individual pig data showing that DMHC increases the density of $A\beta_{42}$-positive neurons in roughly half of the DMHC animals (DMHC control), and that darapladib (DMHC Darapladib) reduces this parameter in DMHC animals to levels comparable to untreated controls (No DMHC). c) Comparison of the density of $A\beta_{42}$-positive smaller pyramidal neurons in the upper cortical layers with that of larger pyramidal neurons that populate deeper layers of the cortex. In both neuronal populations, DMHC increased and darapladib significantly reduced the number of $A\beta_{42}$-positive pyramidal neurons. d) Graph showing that darapladib causes a significant reduction in total $A\beta_{42}$ load in the cerebral cortex of DMHC pigs (DMHC Darapladib) compared to DMHC controls.

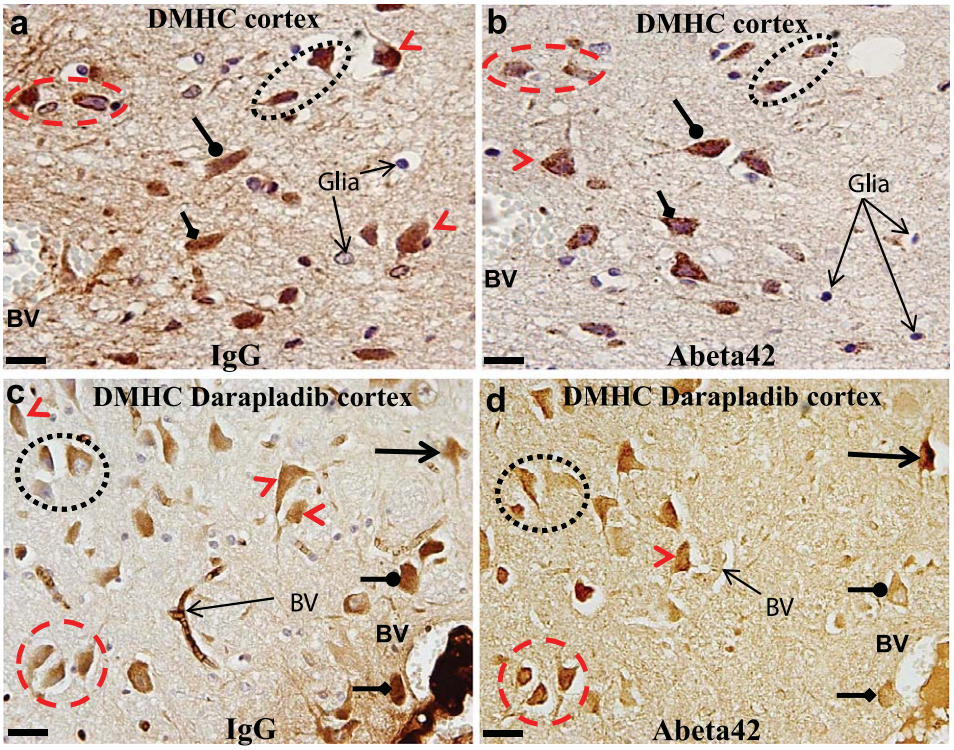

Fig. 7. Cortical pyramidal neurons that bind IgG also accumulate $A\beta_{42}$. Pyramidal neurons in consecutive sections through the cerebral cortex of DMHC controls (a–b) and darapladib-treated DMHC animals (c–d) reveal the co-localization of IgG and $A\beta_{42}$ (encircled and matching arrows). Neurons that failed to demonstrate such co-localization are marked by red arrowheads. BV, blood vessel. Scale bar = 50 μm.

link between DM and HC is now well-recognized [12, 52–54]. This close relationship has prompted speculation that the underlying basis for this risk comes, at least in part, from their well-known deleterious effects on the vasculature, some of which may have their origin in inflammation [12, 14, 55]. In line with this concept, in a previous study investigating human atherosclerosis mechanisms using DMHC swine, darapladib, an inhibitor of lipoprotein-associated phospholipase A2, was found to block the progression of arterial plaques to a higher-risk phenotype by reducing the number of inflammatory macrophages within plaques and curtailing the development and expansion of necrotic cores [44]. During the in-life phase of this study, observations of improved alertness and increased activity of darapladib-treated animals over untreated animals were noted. This, along with the growing recognition of the role of BBB breakdown in the initiation and long-term progression of AD [13, 14, 43, 56], led us to hypothesize that the observed behavioral improvements in darapladib-treated DMHC pigs over untreated DMHC animals may be due to beneficial effects of this drug on the functional integrity of the BBB. This hypothesis prompted the present study using the DMHC pig as a model system. These animals carry the advantage as a particularly relevant model system for studies on neurodegenerative diseases for a number of reasons. First, they have a close similarity in their metabolism and physiology to that of humans. Second, unlike the mouse and rat, pigs have a larger brain size which possesses a vascular hierarchy similar to humans. Lastly, again unlike the mouse and rat, pigs are vulnerable to atherosclerosis and diabetes and develop cardiovascular anomalies that closely mimic, in both type and extent, those that are now reaching epidemic proportions in an aging and obese human population with rampant diabetes [9, 10, 12, 57, 58]. Furthermore, as 70% of diabetic patients also have hypercholesterolemia, the DMHC pig model provides a unique opportunity to study the effects of DM and HC, the two most common co-morbidities [12, 35, 52, 59].

The major findings and implications of the present study are: (1) the demonstration that the condition of DMHC favors increased BBB permeability and the influx of plasma components into the brain tissue, which can disrupt brain homeostasis with possible

consequences to neuronal activity and behavior; (2) that the leakage of IgG from brain blood vessels and its binding to local pyramidal neurons may induce functional disruption and pathological changes in these neurons and may be mechanistically linked to intraneuronal $A\beta_{42}$ deposition in the brain, an early pathological event observed in AD brains; and (3) that alleviation of these deleterious effects of DMHC in the brain by darapladib support the strategy that therapies aimed at the vasculature which block or repair BBB breakdown can have beneficial effects on AD as well as other neurodegenerative diseases. This is particularly true given the fact that most (if not all) of these diseases exhibit inflammation and BBB breakdown as important pathological components at some point during the course of the disease [43].

Chronic BBB breakdown: A largely underrated feature of neurodegenerative diseases

We show here that chronic DMHC in the pig is associated with changes in the brain microvasculature that lead to increased BBB permeability and the influx of plasma components into the brain tissue. Although all vessel subtypes comprising the brain microvasculature were found to exhibit BBB breakdown, arterioles were clearly the primary contributors to the total amount of plasma components that entered into the brain tissue, with the leaked material often forming telltale perivascular, IgG-immunopositive leak clouds. We suspect that this apparent selectivity for arterioles relates to the fact that these vessels, unlike capillaries and venules, are under considerable positive pressure. Thus, even under conditions where the BBB is defective throughout the microvasculature, arterioles would appear to be the major source of extravasated materials.

Although the underlying mechanism(s) leading to the deleterious effects of chronic DMHC on the structure and function of the BBB are unknown, it is likely to be linked to a chronic vascular pathology that evolves as a result of this condition [12–14, 25]. Recently, increasing attention has been given to the role of aging-associated vascular pathologies in the initiation and progression of neurodegenerative diseases, including AD, vascular dementia (now called vascular cognitive impairment), Parkinson's disease, and white matter disease [28, 41, 51, 56, 60–63]. Brain imaging studies in humans and animal models have suggested that cerebrovascular dysfunction is a very early event and may precede cognitive decline and the onset of neurodegenerative changes, and there is evidence that successful treatment of certain vascular risk factors can slow the progression of AD [64, 65]. Breakdown of the BBB appears to be far more common in neurodegenerative diseases than previously thought [37, 43]. In support of this, we and others have detected widespread BBB compromise among human AD and age-matched control brains [40–42, 51, 65–68]. Breach of the BBB in AD brains is accompanied by the influx of many plasma components, including soluble Aβ peptides, complement cascade proteins, serum albumin, and immunoglobulins, into the brain tissue, which can disrupt brain homeostasis [38–40, 45]. The affinity of some of these plasma components (e.g., immunoglobulin, complements, and Aβ peptides) for neuronal and glial cell surfaces may perturb the normal functioning of these cells and even contribute to the well-documented, rampant neurodegeneration and cell death that accompanies neurodegenerative diseases such as AD [42]. In addition, progressive neuronal loss would be expected to secondarily launch local chronic inflammatory responses that persist throughout the disease course, providing conditions that would be expected to exacerbate BBB permeability [30, 69]. Although it has not yet been demonstrated that BBB breakdown can initiate a neurodegenerative disease, it is certainly a major contributing factor to long-term disease progression and may contribute to the spread of the disease from local sites of pathology [28, 41, 42, 66].

IgG leaks through a permeable BBB and binds selectively to pyramidal neurons

The present study also shows that pyramidal neurons located within or near perivascular leak clouds were often strongly and selectively IgG-positive, suggesting that they possess determinants on their surfaces that can serve as targets for blood-borne antibodies that leak into the brain interstitium. In DMHC pig brains, many of the more intensely IgG-positive neurons displayed "corkscrew dendrites", indicative of dendrite collapse and retraction. Despite this, no evidence of cell death was noted in any of the subject groups, suggesting that our pig model may be exhibiting pathological features consistent with only the earliest stages of a neurodegenerative disease where neurons are functionally compromised but not yet degenerating and dying. The absence of amyloid plaques in the brain parenchyma also supports this notion. Inhibition of BBB breakdown could potentially explain the observed behavioral improvements seen in the darapladib-treated, DMHC animals compared to untreated DMHC controls. The reason for the selectivity of IgG for cortical pyramidal neurons is not

known. However, our recent studies have shown that IgG-positive cells, especially pyramidal neurons, are also both universally present and abundant in the cerebral cortex and hippocampus/entorhinal cortex of AD brains, and are most prevalent in brain regions displaying AD-associated pathological features, including intraneuronal $A\beta_{42}$ deposition and amyloid plaques [42]. These observations further support a temporal and spatial link between the occurrence of BBB breakdown and ongoing and evolving AD pathology. In addition, these findings also suggest that, upon BBB breakdown, such neurons are chronically accessible to blood-borne, brain-reactive autoantibodies that leak into the brain tissue and bind to these neurons throughout the course of the disease [39, 41, 42].

In the present study, we confirmed the presence of abundant brain-reactive autoantibodies in pig sera using western analysis. Our data suggest that most brain-reactive autoantibodies persisted in pig sera throughout the treatment period, although the titers of individual autoantibodies varied somewhat and a few additional autoantibodies were added or deleted during the treatment period. Abundant brain-reactive autoantibodies have also been detected in human sera, including sera from AD patients, Parkinson's disease patients, age-matched controls, and younger healthy individuals [42, 45, 70, 71]. In a recent study of human sera using protein microarrays, we have demonstrated the ubiquitous presence of thousands of autoantibodies in the blood and have demonstrated that the increased presence of some autoantibodies may be in response to ongoing pathology, and these disease-specific autoantibodies appear to be of diagnostic value [70, 71]. Taken together, the combination of BBB breakdown and the presence and chronic binding of abundant and potent neuron-binding autoantibodies to neurons could play a role in triggering the neuronal pathologies seen in a number of neurodegenerative diseases, including AD. This would also provide a reasonable explanation for the fact that most neurodegenerative diseases occur in the elderly who are more vulnerable to brain microvascular disease and thus BBB compromise [41, 51, 60, 66, 72]. Lastly, DM and HC are common conditions in the elderly and are likely to be key contributors to the vascular compromise seen in this population [12, 16, 34, 35, 53].

DMHC increases and darapladib reduces BBB leaks in the pig brain

The present study shows that DMHC causes increased BBB permeability throughout the brain microvasculature as evidenced by the increased presence of perivascular, IgG-positive leak clouds and the influx of IgG into the brain parenchyma. DMHC-mediated exacerbation of BBB permeability could occur in several ways. For example, a sustained disruption of the BBB-associated tight junctions between adjacent vascular endothelial cells at the leak site along with dysfunction and/or degradation of the endothelial cell basement membrane and detachment of astrocytic end-feet from the outer wall of the blood vessels are all events that could possibly initiate BBB disruption focally and stochastically. Once initiated, this microvascular pathology could spread bidirectionally along the length of the vessel, resulting in an increase in the number of vascular leaks as observed in DMHC pig brains. Although the initiating events of this process are still unknown, it is widely believed that disruption of tight junctions between adjacent vascular endothelial cells, often referred to as the structural correlate of the BBB, is required for increased BBB permeability. A recent study in the rat showed that streptozotocin-induced DM resulted in decreased occludin expression at both mRNA and protein levels in vascular endothelial cells in the spinal cord [73]. This down-regulation appeared to correlate with the course of the disease and was proposed as a possible causal factor of the DM-induced increase of BBB permeability. However, contrasting results were reported in another study on the blood-retinal barrier [74]. In this case, when transcription levels of genes related to BBB tight junctions were compared in the entire rat retina and bovine retinal endothelial cells after 6 and 12 weeks of streptozotocin-induced DM, endothelial cell genes for occludin and claudin-5 initially showed a transient downregulation, followed by a long-term upregulation. It is conceivable that this response sequence may reflect a damage-response mechanism whereby functional disruption of the BBB induces a compensatory upregulation of tight junction protein expression. Interestingly, DM has been shown to disturb microvascular function through mechanisms that include activation of protein kinase C, production of excessive reactive oxygen species, and cellular activation of the receptor for advanced glycation endproducts [14, 75, 76]. Lastly, the activity of matrix metalloproteinases (MMPs) is also increased in DM patients, and this is associated with a degradation of tight junctions [16, 77]. Studies on rats with streptozotocin-induced DM showed increased plasma MMP activity coincident with increased BBB permeability, raising the possibility that the observed BBB permeability changes are due to elevated plasma MMP activity and MMP-mediated

degradation of BBB-associated tight junctions [16, 77]. Although one or more of these mechanisms may be operating, we have found that darapladib treatment reduced BBB permeability to levels comparable to normal non-DMHC controls. Surprisingly, rather than reducing the number of arteriolar leaks, darapladib instead appeared to be more effective in reducing the amount of material arising from each leak. We suggest that this effect may be due to the action of darapladib in curtailing the progression of existing pathology. In support of this possibility, our previous study on atherosclerosis using the DMHC pig model showed that darapladib was most effective in blocking the pathological advancement of existing atherosclerotic lesions to a more complex phenotype [44].

The selective accumulation of $A\beta_{42}$ in pyramidal neurons is increased by DMHC and reduced by darapladib in DMHC animals

The present study also shows that the $A\beta_{42}$ peptide is abundantly present in the cerebral cortex of the DMHC porcine brain. We consistently found that nearly all $A\beta_{42}$ detectable within the brain was confined to pyramidal neurons, the dominant cell type in the cerebral cortex. A small amount of additional $A\beta_{42}$ was observed in a few arterioles exhibiting cerebrovascular amyloid angiopathy. The reason for the remarkable selectivity of $A\beta_{42}$ for pyramidal neurons is unknown, but it is interesting to note that these are the same neurons that are well-known to accumulate excessive amounts of $A\beta_{42}$-positive material in human AD brains [47]. In addition, as shown here, these are also the same neurons that selectively bind IgG released from blood vessels. In a study of a mouse model of BBB breakdown induced by exposure to Pertussis toxin, we have shown that fluorescein-conjugated $A\beta_{42}$ introduced into the blood can leak into the brain interstitium, selectively enter local pyramidal neurons, and accumulate in their lysosomal compartments [40, 42]. In the present study, we found that treatment with darapladib resulted in a significant reduction in the density of $A\beta_{42}$-positive neurons throughout the cerebral cortex of DMHC pigs. We also determined that the effects of DMHC on intraneuronal $A\beta_{42}$ deposition were not uniform among all pigs in the DMHC subject group. DMHC increased the density of $A\beta_{42}$-positive neurons to a similar level in only roughly half of the animals, whereas the remainder of DMHC animals showed lower densities of $A\beta_{42}$-positive neurons comparable to the other two subject groups. This suggests that the condition of DMHC does not affect all animals equally. Interestingly, treatment with darapladib resulted in a blocking this DMHC-mediated increase in the density of $A\beta_{42}$-positive neurons in the cerebral cortex, suggesting that it may somehow block conditions that trigger increased $A\beta_{42}$ deposition within the pyramidal neurons. These observations are consistent with the notion that this beneficial effect occurs at the level of the BBB.

Importantly, our demonstration that the binding of IgG and accumulation of $A\beta_{42}$ occurs in the same neuronal subtype and, in fact, in the same neurons as observed in consecutive histological sections raises the interesting possibility that these two events are mechanistically linked. In support of this, we have recently investigated the possible interrelationship between neuronal IgG binding and $A\beta_{42}$ accumulation by testing the effects of human serum autoantibodies on the intraneuronal deposition of soluble, exogenous $A\beta_{42}$ peptide in adult mouse neurons in organotypic brain slice cultures [42]. Chronic binding of human serum autoantibodies to mouse neurons in these cultures was shown to dramatically increase the rate and extent of intraneuronal $A\beta_{42}$ accumulation in the mouse cerebral cortex and hippocampus, brain regions well-known to be targets of AD pathology. Interestingly, the potency of individual sera, as judged by their ability to immunolabel neurons in sections of human brain tissue, correlated well with their capacity to enhance intraneuronal $A\beta_{42}$ peptide accumulation [42].

The exact mechanism by which darapladib exerts the beneficial effects reported here on the functional integrity of the BBB in the pig model is unknown. As for atherosclerosis, it is likely to involve anti-inflammatory effects arising in the walls of blood vessels from inhibition of the activity of Lp-PLA_2. Lp-PLA_2 rapidly degrades polar phospholipids present in oxidized LDL-C, releasing downstream products such as lysophosphatidylcholine species and oxidized fatty acids [78, 79]. These products are thought to drive a cascade of events that promote local chronic inflammation. In the present study, we show that the enhanced BBB permeability observed in DMHC pigs is alleviated by darapladib which also reduces intraneuronal deposition of $A\beta_{42}$. In view of these known effects of darapladib on inhibiting the activity of circulating Lp-PLA_2 and local production of proinflammatory mediators, our findings suggest a link between the release of these mediators within the brain blood vessels and increased BBB permeability. If this proves to be the case, then blocking the production of proinflammatory mediators within blood vessels may prove to be an effective and early therapeutic strategy for the

prevention and/or repair of BBB breakdown that could potentially postpone the onset and slow the progression of AD pathogenesis as well as other neurodegenerative disorders.

Perspectives

It is becoming increasingly clear that breakdown of the BBB contributes to the pathogenesis of neurodegenerative diseases such as AD. Although the contribution of BBB breakdown to the long-term progression of these diseases is generally accepted, its role in triggering neurodegenerative diseases is still in question and much more difficult to demonstrate definitively. In the present study, we provide evidence for a mechanistic link between chronic DM, HC, BBB breakdown, selective IgG binding to neurons, and neuronal Aβ peptide accumulation. Our results suggest that metabolic disorders such as DM and HC can trigger neurodegenerative changes through BBB compromise and $A\beta_{42}$ accumulation. In addition, this study also identifies factors (e.g., darapladib treatment) that can alleviate various neurodegenerative changes instigated by DM and HC. Inhibition or reduction of BBB breakdown has great potential for long-term treatment of neurodegenerative diseases, particularly if the therapeutic intervention is applied early, either before disease onset or at early stages of the disease. The beneficial effects of darapladib on BBB permeability reported here in the pig model bodes well for AD patients as well as individuals with other types of progressive neurodegenerative diseases where inflammation and BBB breakdown are inevitable pathological partners. Of course, early treatment will be necessary or at least potentially the most beneficial, but this will require early disease detection. For example, if darapladib or similarly acting agents can significantly reduce vascular leaks in the elderly brain, this could translate into a delayed disease onset and, later, perhaps a marked reduction in the rate of disease progression. The clinical, caregiving, and financial impact of such an effect cannot be overestimated.

ACKNOWLEDGMENTS

The superb animal husbandry of H. Profka is gratefully acknowledged. These studies were supported by funding from GlaxoSmithKline through an industry-academic alliance via the Alternative Drug Discovery Initiative with the University Of Pennsylvania School Of Medicine.

Authors' disclosures available online (http://www.j-alz.com/disclosures/view.php?id=1638).

REFERENCES

[1] (2012) 2012 Alzheimer's disease facts and figures. *Alzheimers Dement* **8**, 131-168.
[2] Blennow K, de Leon MJ, Zetterberg H (2006) Alzheimer's disease. *Lancet* **368**, 387-403.
[3] Dickson DW (1997) Neuropathological diagnosis of Alzheimer's disease: A perspective from longitudinal clinicopathological studies. *Neurobiol Aging* **18**, S21-S26.
[4] Grundke-Iqbal I, Iqbal K, Tung YC, Quinlan M, Wisniewski HM, Binder LI (1986) Abnormal phosphorylation of the microtubule-associated protein tau (tau) in Alzheimer cytoskeletal pathology. *Proc Natl Acad Sci U S A* **83**, 4913-4917.
[5] Hyman BT, Trojanowski JQ (1997) Consensus recommendations for the postmortem diagnosis of Alzheimer disease from the National Institute on Aging and the Reagan Institute Working Group on diagnostic criteria for the neuropathological assessment of Alzheimer disease. *J Neuropathol Exp Neurol* **56**, 1095-1097.
[6] Mirra SS, Hart MN, Terry RD (1993) Making the diagnosis of Alzheimer's disease. A primer for practicing pathologists. *Arch Pathol Lab Med* **117**, 132-144.
[7] Schubert P, Ogata T, Marchini C, Ferroni S (2001) Glia-related pathomechanisms in Alzheimer's disease: A therapeutic target? *Mech Ageing Dev* **123**, 47-57.
[8] DeKosky ST, Scheff SW (1990) Synapse loss in frontal cortex biopsies in Alzheimer's disease: Correlation with cognitive severity. *Ann Neurol* **27**, 457-464.
[9] Allen KV, Frier BM, Strachan MW (2004) The relationship between type 2 diabetes and cognitive dysfunction: Longitudinal studies and their methodological limitations. *Eur J Pharmacol* **490**, 169-175.
[10] Awad N, Gagnon M, Messier C (2004) The relationship between impaired glucose tolerance, type 2 diabetes, and cognitive function. *J Clin Exp Neuropsychol* **26**, 1044-1080.
[11] Biessels GJ, Staekenborg S, Brunner E, Brayne C, Scheltens P (2006) Risk of dementia in diabetes mellitus: A systematic review. *Lancet Neurol* **5**, 64-74.
[12] Carlsson CM (2010) Type 2 diabetes mellitus, dyslipidemia, and Alzheimer's disease. *J Alzheimers Dis* **20**, 711-722.
[13] Huber JD (2008) Diabetes, cognitive function, and the blood-brain barrier. *Curr Pharm Des* **14**, 1594-1600.
[14] Taguchi A (2009) Vascular factors in diabetes and Alzheimer's disease. *J Alzheimers Dis* **16**, 859-864.
[15] Shepardson NE, Shankar GM, Selkoe DJ (2011) Cholesterol level and statin use in Alzheimer disease: I. Review of epidemiological and preclinical studies. *Arch Neurol* **68**, 1239-1244.
[16] Hawkins BT, Lundeen TF, Norwood KM, Brooks HL, Egleton RD (2007) Increased blood-brain barrier permeability and altered tight junctions in experimental diabetes in the rat: Contribution of hyperglycaemia and matrix metalloproteinases. *Diabetologia* **50**, 202-211.
[17] Ahtiluoto S, Polvikoski T, Peltonen M, Solomon A, Tuomilehto J, Winblad B, Sulkava R, Kivipelto M (2010) Diabetes, Alzheimer disease, and vascular dementia: A population-based neuropathologic study. *Neurology* **75**, 1195-1202.
[18] Leibson CL, Rocca WA, Hanson VA, Cha R, Kokmen E, O'Brien PC, Palumbo PJ (1997) Risk of dementia among per-

sons with diabetes mellitus: A population-based cohort study. *Am J Epidemiol* **145**, 301-308.

[19] Ott A, Stolk RP, Hofman A, van Harskamp F, Grobbee DE, Breteler MM (1996) Association of diabetes mellitus and dementia: The Rotterdam Study. *Diabetologia* **39**, 1392-1397.

[20] Zambon D, Quintana M, Mata P, Alonso R, Benavent J, Cruz-Sanchez F, Gich J, Pocovi M, Civeira F, Capurro S, Bachman D, Sambamurti K, Nicholas J, Pappolla MA (2010) Higher incidence of mild cognitive impairment in familial hypercholesterolemia. *Am J Med* **123**, 267-274.

[21] Whitmer RA, Gunderson EP, Barrett-Connor E, Quesenberry CP Jr, Yaffe K (2005) Obesity in middle age and future risk of dementia: A 27 year longitudinal population based study. *BMJ* **330**, 1360.

[22] Yaffe K, Barrett-Connor E, Lin F, Grady D (2002) Serum lipoprotein levels, statin use, and cognitive function in older women. *Arch Neurol* **59**, 378-384.

[23] Solomon A, Kareholt I, Ngandu T, Winblad B, Nissinen A, Tuomilehto J, Soininen H, Kivipelto M (2007) Serum cholesterol changes after midlife and late-life cognition: Twenty-one-year follow-up study. *Neurology* **68**, 751-756.

[24] de la Torre JC (2004) Is Alzheimer's disease a neurodegenerative or a vascular disorder? Data, dogma, and dialectics. *Lancet Neurol* **3**, 184-190.

[25] Breteler MM (2000) Vascular involvement in cognitive decline and dementia. Epidemiologic evidence from the Rotterdam Study and the Rotterdam Scan Study. *Ann N Y Acad Sci* **903**, 457-465.

[26] Kalaria RN (2010) Vascular basis for brain degeneration: Faltering controls and risk factors for dementia. *Nutr Rev* **68**(Suppl 2), S74-S87.

[27] Thal DR, Grinberg LT, Attems J (2012) Vascular dementia: Different forms of vessel disorders contribute to the development of dementia in the elderly brain. *Exp Gerontol* **47**, 816-824.

[28] Bell RD, Zlokovic BV (2009) Neurovascular mechanisms and blood-brain barrier disorder in Alzheimer's disease. *Acta Neuropathol* **118**, 103-113.

[29] Akiyama H, Barger S, Barnum S, Bradt B, Bauer J, Cole GM, Cooper NR, Eikelenboom P, Emmerling M, Fiebich BL, Finch CE, Frautschy S, Griffin WS, Hampel H, Hull M, Landreth G, Lue L, Mrak R, Mackenzie IR, McGeer PL, O'Banion MK, Pachter J, Pasinetti G, Plata-Salaman C, Rogers J, Rydel R, Shen Y, Streit W, Strohmeyer R, Tooyoma I, Van Muiswinkel FL, Veerhuis R, Walker D, Webster S, Wegrzyniak B, Wenk G, Wyss-Coray T (2000) Inflammation and Alzheimer's disease. *Neurobiol Aging* **21**, 383-421.

[30] Carrano A, Hoozemans JJ, van der Vies SM, van Horssen J, de Vries HE, Rozemuller AJ (2012) Neuroinflammation and blood-brain barrier changes in capillary amyloid angiopathy. *Neurodegener Dis* **10**, 329-331.

[31] Sparks DL, Kuo YM, Roher A, Martin T, Lukas RJ (2000) Alterations of Alzheimer's disease in the cholesterol-fed rabbit, including vascular inflammation. Preliminary observations. *Ann N Y Acad Sci* **903**, 335-344.

[32] Sims-Robinson C, Kim B, Rosko A, Feldman EL (2010) How does diabetes accelerate Alzheimerdisease pathology? *Nat Rev Neurol* **6**, 551-559.

[33] Abbott NJ, Patabendige AA, Dolman DE, Yusof SR, Begley DJ (2010) Structure and function of the blood-brain barrier. *Neurobiol Dis* **37**, 13-25.

[34] Bowman GL, Kaye JA, Quinn JF (2012) Dyslipidemia and blood-brain barrier integrity in Alzheimer's disease. *Curr Gerontol Geriatr Res* **2012**, 184042.

[35] Craft S (2009) The role of metabolic disorders in Alzheimer disease and vascular dementia: Two roads converged. *Arch Neurol* **66**, 300-305.

[36] Gloor SM, Wachtel M, Bolliger MF, Ishihara H, Landmann R, Frei K (2001) Molecular and cellular permeability control at the blood-brain barrier. *Brain Res Brain Res Rev* **36**, 258-264.

[37] Zlokovic BV (2008) The blood-brain barrier in health and chronic neurodegenerative disorders. *Neuron* **57**, 178-201.

[38] Alafuzoff I, Adolfsson R, Grundke-Iqbal I, Winblad B (1985) Perivascular deposits of serum proteins in cerebral cortex in vascular dementia. *Acta Neuropathol* **66**, 292-298.

[39] Alafuzoff I, Adolfsson R, Grundke-Iqbal I, Winblad B (1987) Blood-brain barrier in Alzheimer dementia and in non-demented elderly. An immunocytochemical study. *Acta Neuropathol* **73**, 160-166.

[40] Clifford PM, Zarrabi S, Siu G, Kinsler KJ, Kosciuk MC, Venkataraman V, D'Andrea MR, Dinsmore S, Nagele RG (2007) Abeta peptides can enter the brain through a defective blood-brain barrier and bind selectively to neurons. *Brain Res* **1142**, 223-236.

[41] Mooradian AD (1988) Effect of aging on the blood-brain barrier. *Neurobiol Aging* **9**, 31-39.

[42] Nagele RG, Clifford PM, Siu G, Levin EC, Acharya NK, Han M, Kosciuk MC, Venkataraman V, Zavareh S, Zarrabi S, Kinsler K, Thaker NG, Nagele EP, Dash J, Wang HY, Levitas A (2011) Brain-reactive autoantibodies prevalent in human sera increase intraneuronal amyloid-beta (1-42) deposition. *J Alzheimers Dis* **25**, 605-622.

[43] Weiss N, Miller F, Cazaubon S, Couraud PO (2009) The blood-brain barrier in brain homeostasis and neurological diseases. *Biochim Biophys Acta* **1788**, 842-857.

[44] Wilensky RL, Shi Y, Mohler ER 3rd, Hamamdzic D, Burgert ME, Li J, Postle A, Fenning RS, Bollinger JG, Hoffman BE, Pelchovitz DJ, Yang J, Mirabile RC, Webb CL, Zhang L, Zhang P, Gelb MH, Walker MC, Zalewski A, Macphee CH (2008) Inhibition of lipoprotein-associated phospholipase A2 reduces complex coronary atherosclerotic plaque development. *Nat Med* **14**, 1059-1066.

[45] Levin EC, Acharya NK, Han M, Zavareh SB, Sedeyn JC, Venkataraman V, Nagele RG (2010) Brain-reactive autoantibodies are nearly ubiquitous in human sera and may be linked to pathology in the context of blood-brain barrier breakdown. *Brain Res* **1345**, 221-232.

[46] D'Andrea MR, Nagele RG, Wang HY, Peterson PA, Lee DH (2001) Evidence that neurones accumulating amyloid can undergo lysis to form amyloid plaques in Alzheimer's disease. *Histopathology* **38**, 120-134.

[47] Nagele RG, D'Andrea MR, Anderson WJ, Wang HY (2002) Intracellular accumulation of beta-amyloid (1-42) in neurons is facilitated by the alpha 7 nicotinic acetylcholine receptor in Alzheimer's disease. *Neuroscience* **110**, 199-211.

[48] Onul A, Colvard MD, Paradise WA, Elseth KM, Vesper BJ, Gouvas E, Deliu Z, Garcia KD, Pestle WJ, Radosevich JA (2012) Application of immunohistochemical staining to detect antigen destruction as a measure of tissue damage. *J Histochem Cytochem* **60**, 683-693.

[49] Nunomura A, Tamaoki T, Tanaka K, Motohashi N, Nakamura M, Hayashi T, Yamaguchi H, Shimohama S, Lee HG, Zhu X, Smith MA, Perry G (2010) Intraneuronal amyloid beta accumulation and oxidative damage to nucleic acids in Alzheimer disease. *Neurobiol Dis* **37**, 731-737.

[50] Dumont M, Ho DJ, Calingasan NY, Xu H, Gibson G, Beal MF (2009) Mitochondrial dihydrolipoyl succinyltransferase deficiency accelerates amyloid pathology and memory deficit in

a transgenic mouse model of amyloid deposition. *Free Radic Biol Med* **47**, 1019-1027.

[51] Mooradian AD (1994) Potential mechanisms of the age-related changes in the blood-brain barrier. *Neurobiol Aging* **15**, 751-755; discussion 761-752, 767.

[52] Moroz N, Tong M, Longato L, Xu H, de la Monte SM (2008) Limited Alzheimer-type neurodegeneration in experimental obesity and type 2 diabetes mellitus. *J Alzheimers Dis* **15**, 29-44.

[53] Jiang X, Guo M, Su J, Lu B, Ma D, Zhang R, Yang L, Wang Q, Ma Y, Fan Y (2012) Simvastatin blocks blood-brain barrier disruptions induced by elevated cholesterol both *in vivo* and *in vitro*. *Int J Alzheimers Dis* **2012**, 1-7.

[54] Luchsinger JA, Gustafson DR (2009) Adiposity, type 2 diabetes, and Alzheimer's disease. *J Alzheimers Dis* **16**, 693-704.

[55] Li J, Wang YJ, Zhang M, Xu ZQ, Gao CY, Fang CQ, Yan JC, Zhou HD (2011) Vascular risk factors promote conversion from mild cognitive impairment to Alzheimer disease. *Neurology* **76**, 1485-1491.

[56] Viggars AP, Wharton SB, Simpson JE, Matthews FE, Brayne C, Savva GM, Garwood C, Drew D, Shaw PJ, Ince PG (2011) Alterations in the blood brain barrier in ageing cerebral cortex in relationship to Alzheimer-type pathology: A study in the MRC-CFAS population neuropathology cohort. *Neurosci Lett* **505**, 25-30.

[57] Matsuzaki T, Sasaki K, Hata J, Hirakawa Y, Fujimi K, Ninomiya T, Suzuki SO, Kanba S, Kiyohara Y, Iwaki T (2011) Association of Alzheimer disease pathology with abnormal lipid metabolism: The Hisayama Study. *Neurology* **77**, 1068-1075.

[58] Ohara T, Doi Y, Ninomiya T, Hirakawa Y, Hata J, Iwaki T, Kanba S, Kiyohara Y (2011) Glucose tolerance status and risk of dementia in the community: The Hisayama study. *Neurology* **77**, 1126-1134.

[59] Harris MI (1991) Hypercholesterolemia in diabetes and glucose intolerance in the U.S. population. *Diabetes Care* **14**, 366-374.

[60] Buee L, Hof PR, Delacourte A (1997) Brain microvascular changes in Alzheimer's disease and other dementias. *Ann N Y Acad Sci* **826**, 7-24.

[61] Helzner EP, Luchsinger JA, Scarmeas N, Cosentino S, Brickman AM, Glymour MM, Stern Y (2009) Contribution of vascular risk factors to the progression in Alzheimer disease. *Arch Neurol* **66**, 343-348.

[62] Kalaria RN (1996) Cerebral vessels in ageing and Alzheimer's disease. *Pharmacol Ther* **72**, 193-214.

[63] Kleine TO, Hackler R, Zofel P (1993) Age-related alterations of the blood-brain-barrier (BBB) permeability to protein molecules of different size. *Z Gerontol* **26**, 256-259.

[64] Li G, Shofer JB, Rhew IC, Kukull WA, Peskind ER, McCormick W, Bowen JD, Schellenberg GD, Crane PK, Breitner JC, Larson EB (2010) Age-varying association between statin use and incident Alzheimer's disease. *J Am Geriatr Soc* **58**, 1311-1317.

[65] Ujiie M, Dickstein DL, Carlow DA, Jefferies WA (2003) Blood-brain barrier permeability precedes senile plaque formation in an Alzheimer disease model. *Microcirculation* **10**, 463-470.

[66] Farrall AJ, Wardlaw JM (2009) Blood-brain barrier: Ageing and microvascular disease - systematic review and meta-analysis. *Neurobiol Aging* **30**, 337-352.

[67] Hawkins BT, Davis TP (2005) The blood-brain barrier/neurovascular unit in health and disease. *Pharmacol Rev* **57**, 173-185.

[68] Simpson JE, Wharton SB, Cooper J, Gelsthorpe C, Baxter L, Forster G, Shaw PJ, Savva G, Matthews FE, Brayne C, Ince PG (2010) Alterations of the blood-brain barrier in cerebral white matter lesions in the ageing brain. *Neurosci Lett* **486**, 246-251.

[69] Abbott NJ (2000) Inflammatory mediators and modulation of blood-brain barrier permeability. *Cell Mol Neurobiol* **20**, 131-147.

[70] Nagele E, Han M, Demarshall C, Belinka B, Nagele R (2011) Diagnosis of Alzheimer's disease based on disease-specific autoantibody profiles in human sera. *PLoS One* **6**, e23112.

[71] Han M, Nagele E, DeMarshall C, Acharya N, Nagele R (2012) Diagnosis of Parkinson's disease based on disease-specific autoantibody profiles in human sera. *PLoS One* **7**, e32383.

[72] de la Torre JC (1997) Cerebromicrovascular pathology in Alzheimer's disease compared to normal aging. *Gerontology* **43**, 26-43.

[73] Zhao Y, Liu X, Yu A, Zhou Y, Liu B (2010) Diabetes-related alteration of occludin expression in rat blood-spinal cord barrier. *Cell Biochem Biophys* **58**, 141-145.

[74] Klaassen I, Hughes JM, Vogels IM, Schalkwijk CG, Van Noorden CJ, Schlingemann RO (2009) Altered expression of genes related to blood-retina barrier disruption in streptozotocin-induced diabetes. *Exp Eye Res* **89**, 4-15.

[75] Schreibelt G, Kooij G, Reijerkerk A, van Doorn R, Gringhuis SI, van der Pol S, Weksler BB, Romero IA, Couraud PO, Piontek J, Blasig IE, Dijkstra CD, Ronken E, de Vries HE (2007) Reactive oxygen species alter brain endothelial tight junction dynamics via RhoA, PI3 kinase, and PKB signaling. *FASEB J* **21**, 3666-3676.

[76] Yan SD, Chen X, Fu J, Chen M, Zhu H, Roher A, Slattery T, Zhao L, Nagashima M, Morser J, Migheli A, Nawroth P, Stern D, Schmidt AM (1996) RAGE and amyloid-beta peptide neurotoxicity in Alzheimer's disease. *Nature* **382**, 685-691.

[77] Hartz AM, Bauer B, Soldner EL, Wolf A, Boy S, Backhaus R, Mihaljevic I, Bogdahn U, Klunemann HH, Schuierer G, Schlachetzki F (2012) Amyloid-beta contributes to blood-brain barrier leakage in transgenic human amyloid precursor protein mice and in humans with cerebral amyloid angiopathy. *Stroke* **43**, 514-523.

[78] MacPhee CH, Moores KE, Boyd HF, Dhanak D, Ife RJ, Leach CA, Leake DS, Milliner KJ, Patterson RA, Suckling KE, Tew DG, Hickey DM (1999) Lipoprotein-associated phospholipase A2, platelet-activating factor acetylhydrolase, generates two bioactive products during the oxidation of low-density lipoprotein: Use of a novel inhibitor. *Biochem J* **338**(Pt 2), 479-487.

[79] Rosenson RS, Stafforini DM (2012) Modulation of oxidative stress, inflammation, and atherosclerosis by lipoprotein-associated phospholipase A2. *J Lipid Res* **53**, 1767-1782.